Spurious singularities in the generalized Newton variational method

Barnabás Apagyi and Péter Lévay
Quantum Theory Group, Institute of Physics, Technical University of Budapest, H-1521 Budapest, Hungary

Károly Ladányi
Institute for Theoretical Physics, Roland Eötvös University, H-1088 Budapest, Hungary
(Received 15 July 1991)

The generalized Newton variational method is applied to the static-exchange approximation of the electron–hydrogen-atom scattering. Slater-type basis functions are employed to expand the amplitude density. Spurious singularities are encountered in both scattering processes. The width of the unphysical singularities is broader in the case of singlet scattering. Anomalous poles appear in narrow regions of the scale parameter and are in evident correlation with the zeros of the determinant of the free-particle Green's operator. As a by-product, simple least-squares extension of the generalized Newton variational method is developed in order to avoid spurious singularities and to recognize whether or not the convergence is of secondary nature.

PACS number(s): 03.65.Nk, 34.80.Bm, 02.60.+y

I. INTRODUCTION

The Newton variational method [1] has proved to be an efficient computational tool in different branches of quantum scattering theory. In nuclear physics, for example, it was applied to study the off- and on-shell behavior of the $\underline{T}$-matrix elements of various few-particle reactions [2–6]. In chemical physics, the generalized Newton variational method [7,8] (GNVM) has been formulated recently [9,10] to a stage which should provide a practical method for carrying out three-dimensional quantal calculations for reactive molecular collisions and molecular photoionization processes [7–22].

According to the general classification scheme of the variational methods in scattering theory [23], the GNVM belongs to the Schwinger-type variational procedures. It is based on the Lippman-Schwinger integral equation for the amplitude density [24] being the trial quantity in the generalized Newton functional [8]. Since the amplitude density is a well-localized spatial function [21,24] for distorting potentials inducing reactions in chemical physics, the GNVM requires basis functions selected exclusively from the $\mathcal{L}^2$ space. Another important property of the method is the fact that it explicitly involves the Born term [1]. One would therefore expect the GNVM to perform better at higher scattering energies than at lower ones.

Comparative test calculations [7–12] have shown however that the Newton variational method is capable of providing accurate results also in the dynamically important low-energy regions. These studies have revealed the fundamental properties that the GNVM is practically insensitive to the choice of the different basis sets being in general use, and achieves a fast convergence for all the typical potentials arising in various chemical reaction problems. This so-called robust [12] character of the GNVM makes it potentially a prominent candidate to be employed in the future applications. Therefore, the GNVM deserves to be analyzed further in order to explore its more subtle properties.

It is the purpose of the present investigation to provide additional insight into the performance of the GNVM. Motivated by the facts that (i) there exists a hierarchical relationship [25,26] among the variational functionals due to Kohn, Schwinger, and Newton, (ii) spurious singularities are frequently encountered [27,28] in the applications of the Kohn variational method but less frequently [29–33] in the Schwinger variational method, (iii) no such anomalies have been reported so far in conjunction with the Newton variational method (although a recent development [15] of the $\underline{T}$-matrix version of the GNVM indicates [34] that anomalies have been encountered in previous $\underline{K}$-matrix calculations) , and (iv) there seems to exist a prevalent [2,22] theoretical confidence about the anomaly-free character of the Newton variational method, we have addressed to ourselves the interesting question of theoretical importance: whether or not a GNVM calculation yields spurious singularities for typical potentials when typical sets of basis functions are also being used.

The numerical results of the present paper indicate that there are scattering potentials and basis functions for which the GNVM gives rise to anomalous (i.e., nonphysical) behavior of the calculated $\underline{K}$-matrix elements as a function of the scattering energy. This feature is similar to that observed [27,28] in the application of the Kohn variational method. As a test example we shall consider the static-exchange approximation of the electron–hydrogen-atom scattering. The GNVM calculations will be carried out using Slater-type basis functions characterized by a nonlinear scale parameter.

We shall demonstrate that spurious singularities of the Kohn type do arise in the tangent of the s-wave phase shifts computed by the GNVM for *both* (singlet and triplet) scattering processes. (Note that the Schwinger variational method is free of anomalies in the triplet case.)

The spurious singularities are located in narrow regions of the wave number k and nonlinear parameter α. A pronounced correlation is found to exist between the region of anomalies and the positions of the zero eigenvalues of the matrix of the free-particle Green's function. A stubborn secondary plateau of the $\underline{K}$ matrix computed as a function of α is shown to appear in the singlet case at a particular value of k. This feature, well known [27,31] in the Kohn variational method, may lead one to draw quite a false conclusion about the accuracy of the computed results if only the convergence characteristics are investigated. Both shortcomings (spurious singularities and apparent convergence) can be overcome by applying a simple least-squares extension to the GNVM.

It is important to note that similar anomalies of the GNVM have been encountered by using a large class of local potentials, such as exponential potentials or Yukawa potentials. Also the change of the basis set does not seem to cure this unpleasant feature of the GNVM since the use of exponential basis sets with uniformly distributed scale parameters has resulted in the appearance of spurious singularities similar to those presented in this paper. We emphasize therefore that the validity of some conclusions (see, e.g., Ref. [22]) assuming the anomaly-free character of the Newton variational method should be checked by appropriate methods.

The organization of this paper is as follows. Section II contains the necessary formalism including a least-squares extension of the GNVM which avoids the anomalies. In Sec. III we present the analysis of the results obtained for the static-exchange potential by both the GNVM and its least-squares extension. Some comments are left for Sec. IV.

II. ANALYSIS OF THE GENERALIZED NEWTON VARIATIONAL METHOD

A. Static-exchange approximation

Let us consider the s-wave ($l=0$) elastic scattering of an electron by a hydrogen atom and, as a test case, make use of the simple static-exchange approximation introduced by Erskine and Massey [35]. Employing atomic units (a.u.), and denoting the total energy of the electron–hydrogen-atom system by E, the ground-state energy of the hydrogen atom by E_1 ($E_1=-0.5$a.u.), and the kinetic energy of the scattering electron by $\varepsilon=E-E_1=k^2/2$, the static-exchange approximation of the interaction potential (operator) becomes [35]

$$V=V_1(r)+\mathcal{W}_2(E) , \tag{2.1}$$

where the energy-independent local part is defined by

$$V_1(r)=-\left[\frac{1}{r}+1\right]e^{-2r} , \tag{2.2}$$

and the energy-dependent nonlocal (exchange) operator can be written, in symbolic notation, as

$$\mathcal{W}_2=-\int_0^\infty dr' r w(r,r') r' \tag{2.3}$$

with

$$w(r,r')=4(-1)^S e^{-r}(E-2E_1-r_>^{-1})e^{-r'} . \tag{2.4}$$

Here we have $S=0$ for the singlet scattering process, and the triplet scattering states are characterized by $S=1$. [The symbol $r_>$ in Eq. (2.4) denotes the greater of r,r'.]

B. Lippmann-Schwinger equations

The scattering process above is described by a radial scattering wave function $f_1(r)$ which satisfies the Lippmann-Schwinger equation

$$f_1=\tilde{S}+\mathcal{G}Uf_1 , \tag{2.5}$$

where

$$U=2V \tag{2.6}$$

and $\mathcal{G}$ is the *principal-value* free-particle Green's function which can be written symbolically [8] as

$$\mathcal{G}=-\frac{1}{k}\int_0^\infty dr' \tilde{S}(r_<)\tilde{C}(r_>) \tag{2.7}$$

with

$$\tilde{S}(r)=k^{-1/2}\sin(kr) , \tag{2.8}$$

$$\tilde{C}(r)=k^{-1/2}\cos(kr) . \tag{2.9}$$

[The symbols $r_<$ and $r_>$ in Eq. (2.7) denote, respectively, the lesser and greater of r,r'.]

By defining the radial amplitude density as [24]

$$\zeta_1=Uf_1 , \tag{2.10}$$

the Lippmann-Schwinger equation for the radial amplitude density becomes

$$\zeta_1=U\tilde{S}+U\mathcal{G}\zeta_1 . \tag{2.11}$$

The integral expression for the reactance matrix element K takes the form

$$K=-\langle\tilde{S}|U|f_1\rangle=-\langle\tilde{S}|\zeta_1\rangle , \tag{2.12}$$

which may be written, using Eqs. (2.5) and (2.10) or Eq. (2.11), in the form

$$K=K^{B1}-\langle\tilde{S}|U\mathcal{G}|\zeta_1\rangle , \tag{2.13}$$

where

$$K^{B1}=-\langle\tilde{S}|U|\tilde{S}\rangle \tag{2.14}$$

is the first Born approximation.

The reactance matrix element K can be computed by using a great variety of finite-basis-set expansion methods [8,30] that are based on the Lippmann-Schwinger integral equations. In this paper we make use of the generalized Newton variational method which is based on the Lippmann-Schwinger equation given by Eq. (2.11).

C. Generalized Newton variational method

The GNVM provides a stationary expression for the approximate reactance matrix elements with respect to small changes about the exact solution of the Lippmann-

Schwinger equation (2.11) for the amplitude density. In the following we derive the GNVM from the general method of moments [2,8,30,36] by selecting appropriate basis functions $\bar{\varphi}_i(r)$ and test functions $\tilde{\chi}_i(r)$. [A tilde on the basis (test) functions indicates the freedom we have in selecting different types of the $\mathcal{L}^2$-space functions.]

As a first step, we consider the expansion of the radial amplitude density $\zeta_1(r)$ in terms of a convenient set of basis functions $\bar{\varphi}_j(r)$. The truncated version of this expansion can be written as

$$\tilde{\zeta}_1(r)=\sum_{j=1}^{N} a_j\bar{\varphi}_j(r) . \tag{2.15}$$

By substituting $\tilde{\zeta}_1(r)$ into the Lippmann-Schwinger equation (2.11), we have

$$(1-U\mathcal{G})\tilde{\zeta}_1-U\tilde{S}=\tilde{\Delta}_1 , \tag{2.16}$$

where the deviation $\tilde{\Delta}_1(r)$ is related to the error of the approximate radial amplitude density $\tilde{\zeta}_1(r)$. Since the amplitude density belongs [21,24] to the $\mathcal{L}^2$ space for the interaction potential defined by Eq. (2.1), we adopt, as basis functions, a set of (nonorthogonal) square-integrable Slater-type functions:

$$\bar{\varphi}_j(r)=A_j r^j e^{-\alpha r}, \quad j=1,2,\ldots,N . \tag{2.17}$$

Here α is a (real) nonlinear scale parameter characterizing the basis and the normalization factors are denoted by A_j.

The next step is the selection of the appropriate test function $\tilde{\chi}_i(r)$. To arrive at the GNVM expression for the $\underline{K}$-matrix element the test functions have to be chosen as follows:

$$\tilde{\chi}_i(r)=\mathcal{G}\bar{\varphi}_i(r) . \tag{2.18}$$

We proceed by fixing N projections of the deviation vector $\tilde{\Delta}_1$ in the test function space at zero:

$$\langle\tilde{\chi}_i|\tilde{\Delta}_1\rangle=0, \quad i=1,2,\ldots,N . \tag{2.19}$$

Equation (2.19) can also be written as

$$\sum_{j=1}^{N} X_{ij}a_j=\langle\tilde{\chi}_i|U|\tilde{S}\rangle , \tag{2.20}$$

where $i=1,\ldots,N$ and

$$X_{ij}=\langle\bar{\varphi}_i|\mathcal{G}-\mathcal{G}U\mathcal{G}|\bar{\varphi}_j\rangle . \tag{2.21}$$

Equation (2.20) is a system of linear inhomogeneous algebraic equations which determines the expansion coefficient a_j according to the general method of moments.

The last step is to calculate the approximate reactance matrix element $\tilde{K}$ by substituting Eq. (2.15) into Eq. (2.13). One obtains

$$\tilde{K}^{(S)}_{\mathrm{GN}}(N;k,\alpha)=K^{B1}-\sum_{j=1}^{N}\langle\tilde{S}|U\mathcal{G}|\bar{\varphi}_j\rangle a_j , \tag{2.22}$$

where the upper index (in parenthesis) refers to the fact that the interaction potential U depends on the quantum number S which takes the values $S=0$ for singlet scattering and $S=1$ for triplet collision. Equations (2.20) and (2.22) imply

$$\tilde{K}^{(S)}_{\mathrm{GN}}(N;k,\alpha)=K^{B1}-\sum_{i,j=1}^{N}\langle\tilde{S}|U\mathcal{G}|\bar{\varphi}_j\rangle(\underline{X}^{-1})_{ji}\langle\bar{\varphi}_i|\mathcal{G}U|\tilde{S}\rangle , \tag{2.23}$$

where $\underline{X}^{-1}$ denotes the inverse of the $\underline{N}\times\underline{N}$ matrix defined by Eq. (2.21). A comparison of Eq. (2.23) with Eq. (78) of Ref. [8] shows that $\tilde{K}^{(S)}_{\mathrm{GN}}$ is the well-known GNVM expression for the approximate reactance matrix element being variationally correct to second-order errors in the trial amplitude density given by Eq. (2.15).

D. Singularities

To explore the singularity structure of the matrix element $\tilde{K}$, Eq. (2.23), it will be convenient [30] to denote the determinant of the $\underline{N}\times\underline{N}$ matrix $\underline{X}$ as follows:

$$\bar{X}(N;k,\alpha)=\det|X_{ij}| . \tag{2.24}$$

Equation (2.23) shows that a singular behavior of $\tilde{K}$ can be expected near the real wave number $k=k_0^{(N)}$ for which

$$\bar{X}(N;k_0^{(N)},\alpha)=0 . \tag{2.25}$$

By computing $k=k_0^{(N)}$ at many values of α (or vice versa), we obtain the function $k_0^{(N)}(\alpha)$. Since the zeros of the determinant $\bar{X}$ are located along the curve(s) $k_0^{(N)}(\alpha)$, it will be convenient to rewrite Eq. (2.25) in the form

$$\bar{X}(N;k_0^{(N)}(\alpha))=0 . \tag{2.26}$$

In order to have a deeper insight into the structure of the singularities of the GNVM, it will be useful to introduce the notation

$$\bar{G}(N;k,\alpha)=\det|G_{ij}|, \quad i,j=1,2,\ldots N \tag{2.27}$$

for the determinant of the matrix elements

$$G_{ij}=\langle\bar{\varphi}_i|\mathcal{G}|\bar{\varphi}_j\rangle \tag{2.28}$$

of the free-particle Green's function defined by Eq. (2.7).

Of course, the matrix $\underline{G}$ may have zero eigenvalues for particular values of α and k. One therefore introduces the function $k_1^{(N)}(\alpha)$, which is related to the zeros of the determinant $\bar{G}(N;k,\alpha)$ by writing

$$\bar{G}(N;k_1^{(N)}(\alpha))=0 . \tag{2.29}$$

Both Eqs. (2.26) and (2.29) can be solved by the same numerical procedure; the solutions of Eq. (2.26) define the function $k_0^{(N)}(\alpha)$, those of Eq. (2.29) prescribe the function $k_1^{(N)}(\alpha)$.

Our numerical calculations show that, using Slater-type basis functions defined by Eq. (2.17), there exists a pronounced correlation between the functions $k_0^{(N)}(\alpha)$ and $k_1^{(N)}(\alpha)$ [cf. Fig. 2]. Since the function $k_1^{(N)}(\alpha)$ has nothing to do with the physical singularities of the $\underline{K}$ ma-

trix, this remarkable correlation between the roots of $\bar{X}(N;k,\alpha)$ and $\bar{G}(N;k,\alpha)$ may indicate the existence of *spurious* singularities of the approximate reactance matrix element computed by the GNVM as given by Eq. (2.23). In the discussion of Sec. III we shall see indeed that the presence of the correlating zeros of the determinants related to the operators $\mathcal{G}-\mathcal{G}U\mathcal{G}$ and $\mathcal{G}$ does in fact give rise to the appearance of spurious singularities of Kohn-type in the GNVM reactance matrix elements.

In order to avoid the spurious singularities of the GNVM one may apply the method proposed by Winstead and McKoy [32] to remove the anomalies of the Schwinger variational method. Here we make use of a least-squares procedure for this purpose along the lines discussed in Ref. [30].

E. Least-squares extension of the GNVM

Let us consider the integral equation

$$(1-U\mathcal{G})\zeta-\tilde{a}_{-1}U\tilde{S}=0 \ . \tag{2.30}$$

Here the coefficient $\tilde{a}_{-1}$ is different from zero and independent of r, otherwise arbitrary. If the value of $\tilde{a}_{-1}$ is fixed at $\tilde{a}_{-1}=1$, then the solution of Eq. (2.30) is $\zeta=\zeta_1$, satisfying the Lippmann-Schwinger equation (2.11).

The radial amplitude density $\zeta(r)$ can be expanded in terms of Slater-type basis functions $\tilde{\varphi}_j(r)$, $j=1,2,\ldots,N,\ldots$, defined by Eq. (2.17). The truncated version of this expansion can be written, similarly to Eq. (2.15), as

$$\tilde{\zeta}=\sum_{j=1}^{N}\tilde{a}_j\tilde{\varphi}_j(r) \ . \tag{2.31}$$

By replacing the radial amplitude density ζ with the approximation $\tilde{\zeta}$, one defines the deviation vector as

$$\Delta(r)=(1-U\mathcal{G})\tilde{\zeta}-\tilde{a}_{-1}U\tilde{S} \ , \tag{2.32}$$

which also depends on the linear parameters $\tilde{a}_{-1},\tilde{a}_1,\tilde{a}_2,\ldots,\tilde{a}_N$.

We next turn to a definition of the measure of the error of the radial amplitude density $\tilde{\zeta}(r)$ in a sufficiently large [$(N+p)$-dimensional] subspace spanned by the test functions $\tilde{\chi}_h=\mathcal{G}\tilde{\varphi}_h$, $h=1,\ldots,N,\ldots,N+p$. This definition can be expressed as [30,37–39]

$$\lambda[\tilde{\zeta}]=\frac{\sum_{h,h'=1}^{N+p}\langle\Delta|\tilde{\chi}_h\rangle w_{hh'}\langle\tilde{\chi}_{h'}|\Delta\rangle}{\tilde{a}^{*}_{-1}\tilde{a}_{-1}} \ , \tag{2.33}$$

with

$$p\geq 2 \ . \tag{2.34}$$

Here the weight matrix $\underline{w}$ is real, symmetric and all the eigenvalues of $\underline{w}$ are larger than zero. For simplicity we shall choose

$$w_{hh'}=\delta_{hh'} \ . \tag{2.35}$$

The variational functional $\lambda[\tilde{\zeta}]$ is positive semidefinite by construction, and we have

$$\lambda[\zeta]=0 \ . \tag{2.36}$$

By variation of $\lambda[\tilde{\zeta}]$ with respect to the linear parameters $\tilde{a}_{-1}$ and $\tilde{a}_j, j=1,\ldots N$, we obtain a simple eigenvalue problem. As a next step, we normalize the eigenvector by setting

$$\tilde{a}_{-1}=1 \ . \tag{2.37}$$

The final result is the system of linear inhomogeneus algebraic equations for the coefficients $\tilde{a}_j$, $j=1,\ldots,N$. These equations can be written in the form given by

$$\sum_{j=1}^{N}L_{ij}\tilde{a}_j=d_i, \quad i=1,2,\ldots,N \tag{2.38}$$

where

$$L_{ij}=\sum_{h=1}^{N+p}X_{ih}X_{hj} \tag{2.39}$$

and

$$d_i=\sum_{h=1}^{N+p}X_{ih}\langle\tilde{\chi}_h|U|\tilde{S}\rangle \ . \tag{2.40}$$

In addition, the formula of the eigenvalue $\lambda=\lambda_{\mathrm{LN}}^{(S)}$ becomes

$$\lambda_{\mathrm{LN}}^{(S)}=\sum_{h=1}^{N+p}\langle\tilde{S}|U|\tilde{\chi}_h\rangle\langle\tilde{\chi}_h|U|\tilde{S}\rangle-\sum_{j,i=1}^{N}d_j^{*}(\underline{L}^{-1})_{ji}d_i \ . \tag{2.41}$$

The approximate reactance matrix element $\tilde{K}_{\mathrm{LN}}^{(S)}$ can be calculated by substituting Eq. (2.31) into Eq. (2.13). One obtains

$$\tilde{K}_{\mathrm{LN}}^{(S)}=K^{B1}-\sum_{j=1}^{N}\langle\tilde{S}|U\mathcal{G}|\tilde{\varphi}_j\rangle\tilde{a}_j \ , \tag{2.42}$$

which depends also on the parameters N,p,α, and the wave number k. Equations (2.38) and (2.42) imply

$$\tilde{K}_{\mathrm{LN}}^{(S)}(N,p;k,\alpha)=K^{B1}-\sum_{j,i=1}^{N}\langle\tilde{S}|U\mathcal{G}|\tilde{\varphi}_j\rangle(\underline{L}^{-1})_{ji}d_i \ . \tag{2.43}$$

For $p=0$, one obtains [by inspecting Eqs. (2.23), (2.39), (2.40), and (2.43)] the equality

$$\tilde{K}_{\mathrm{LN}}^{(S)}(N,p=0;k,\alpha)=\tilde{K}_{\mathrm{GN}}^{(S)}(N;k,\alpha) \ . \tag{2.44}$$

Therefore, Eq. (2.43) may be considered as the approximate reactance matrix element obtained by the least-squares extension for the generalized Newton variational method (LNVM).

For $p\geq 2$, on the other hand, the eigenvalues of the Hermitian matrix $\underline{L}$ are, by construction, non-negative. Therefore Eq. (2.43) may exhibit a wider stability region [i.e., interval of the scale parameter α where the function $\tilde{K}_{\mathrm{LN}}^{(S)}(\alpha)$ at fixed values of N, p, and k is almost constant] than the original GNVM formula Eq. (2.23) (cf. Fig. 1).

All our LNVM calculations will be carried out by choosing

$$p=5\ . \tag{2.45}$$

It is also worth noting that the expression of $\tilde{K}^{(S)}_{LN}$ is constructed from the same type of matrix elements as that of the original $\tilde{K}^{(S)}_{GN}$ itself [cf. Eqs. (2.43), (2.40), and (2.39) with Eqs. (2.23) and (2.21)]. In addition, useful information can be obtained about the accuracy of the calculation by also monitoring the eigenvalue $\lambda^{(S)}_{LN}$ given by Eq. (2.41). This feature of the LNVM might prove helpful when, at different sets of the technical parameters (say, N, α), the GNVM yields different quantitative results of similar quality (convergence and stability) for the *same* physical quantity (say, $\underline{K}$ matrix). In this case one may accept the result which belongs to the smallest eigenvalue $\lambda^{(S)}_{LN}$ of the LNVM calculations. An example for such a pathological situation will also be shown in Sec. III (cf. Fig. 4 and Tables I–III).

III. RESULTS AND ANALYSIS

A. Triplet scattering ($S=1$)

The Newton formula, Eq. (2.23), and its least-squares variant, Eq. (2.43), can be applied to calculate the reactance matrix elements $\tilde{K}^{(1)}_{YN}$ ($Y=G,L$) of the triplet scattering process at the fixed wave number $k=0.5$ a.u. Let us employ five basis functions ($N=5$), ten test functions ($p=5$), and perform the calculations at many values of α within the range $0.7\le\alpha\le 9$.

Figure 1 shows the results where the functions $\tilde{K}^{(1)}_{GN}(\alpha)=\tilde{K}^{(1)}_{GN}(5;0.5,\alpha)$ and $\tilde{K}^{(1)}_{LN}(\alpha)=\tilde{K}^{(1)}_{LN}(5,5;0.5,\alpha)$ are depicted, respectively, by the dashed and solid curves. Between the two vertical dash-dotted lines (indicating a change of scale around $\alpha\approx 1.21$), one observes steep spurious branches of the GNVM reactance matrix element which clearly show the presence of an anomalous pole in the GNVM calculation for the triplet scattering process. This is to be contrasted with the results obtained [29] by using the Schwinger variational method which is free of anomalies for the triplet case. The anomalous singularities of the GNVM can be avoided by the least-squares method (LNVM) of Sec. II, as shown by the solid curve of Fig. 1. Also clearly seen in the figure is that the LNVM results are less sensitive to the choice of the nonlinear scale parameter α of the basis functions given by Eq. (2.17). We note that three spurious singularities of similar subtle structure can be found in the omitted region $0<\alpha<0.7$ of Fig 1. The location of all the singularities of the GNVM calculations related to the triplet scattering process can be found in the next figure.

Figure 2 exhibits the pole structure of the GNVM reactance matrix elements at $S=1$ and $N=5$. The solid curves of Fig. 2 represent the function $k_0^{(5)}(\alpha)$ prescribing the (possible) poles of the reactance matrix elements $\tilde{K}^{(1)}_{GN}(5;0.5,\alpha)$. [The function $k_0^{(5)}(\alpha)$ can be obtained by solving Eq. (2.26).] One observes in Fig. 2 a horizontal trend which consists of five pieces and nicely shows the position of the true singularity at $k\approx 0.8350$ a.u. This horizontal formation is disrupted by sudden changes due to avoided crossing into the spurious branches of the function $k_0^{(5)}(\alpha)$. Figure 2 can thus be used to establish those corresponding values of the wave number k and nonlinear parameter α which should be avoided in the GNVM calculation with five basis functions for the triplet scattering. Fixing the wave number at $k=0.5$ a.u., for example, one should avoid the use of the narrow regions around $\alpha\approx 0.17593$, 0.37796, 0.65275, and 1.20874. [The fifth forbidden value of α given by the prescription $k_0^{(5)}(\alpha)=0.5$ a.u. lies at $\alpha\approx 24.16$, far out of the reasonable α region and is therefore not included in Fig. 2.] One observes also in Fig. 2 that the five spurious branches of $k_0^{(5)}$ are in an obvious correlation with the five dashed straight lines of the function $k_1^{(5)}(\alpha)$ defined

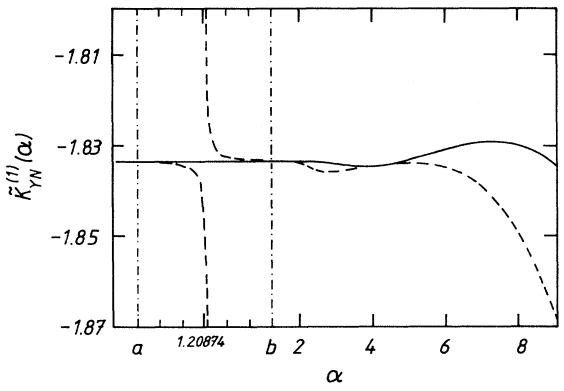

FIG. 1. Reactance matrix elements $\tilde{K}^{(S)}_{YN}$ computed by the generalized Newton variational method ($Y=G$, dashed curves) and its least-squares extension ($Y=L$, solid curves) for the triplet scattering process ($S=1$) at fixed wave number $k=0.5$ a.u. using basis-set size $N=5$, vs the nonlinear scale parameter α within the range $0.7\le\alpha\le 9$. A spurious GNVM singularity appears between the two dash-dotted vertical lines indicating a change of scale in the interval $[a,b]$ with $a=1.208\,71$ and $b=1.208\,77$.

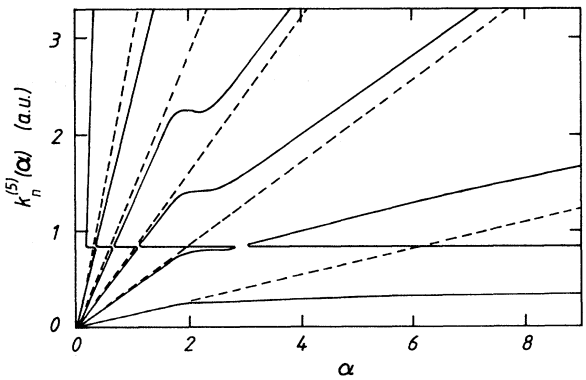

FIG. 2. The wave numbers $k_n^{(5)}(n=0,1)$ vs α. The function $k_0^{(5)}(\alpha)$ is depicted by the solid curves indicating the singular behavior of the GNVM results for triplet scattering ($S=1$). [See Eqs. (2.23) and (2.26).] The dashed lines represent the function $k_1^{(5)}(\alpha)$ which is associated with the zero eigenvalues of the matrix G_{ij} via Eq. (2.29). Both functions were obtained at basis-set size $N=5$.

by Eq. (2.29), representing the zero eigenvalues of the matrix G_{ij}. This apparent correlation is disturbed by the presence of the true singularity line at $k \approx 0.8350$ a.u. producing also the avoided crossings within the function $k_0^{(5)}(\alpha)$ itself.

Our analytical and numerical experiences have shown that the conclusions drawn from Fig. 2 are true for all possible values of N. Using N Slater-type basis functions, the wave numbers $k_1^{(N)}(\alpha)$ [indicating the zero positions of the determinant $\bar{G}$ via Eq. (2.29)] are located along N straight lines starting from the origin. To these N straight lines there belong N spurious branches of the function $k_0^{(N)}(\alpha)$ which prescribe the singularities of the GNVM reactance matrix element. The correlation between the corresponding lines of $k_1^{(N)}$ and $k_0^{(N)}$ is disturbed in the region of the physical singularities induced by the interaction term U governing the scattering process. The presence of the physical singularities thus generates avoided crossings in the function $k_0^{(N)}(\alpha)$. We have found that the correlation between the functions $k_1^{(N)}(\alpha)$ and $k_0^{(N)}(\alpha)$ is stronger for the singlet potential (and also for the attractive Yukawa and exponential potentials) than for the triplet interaction term as shown by Fig. 2.

B. Singlet scattering ($S=0$)

The general observations above can also be used to predict the regions of the wave numbers k at which the GNVM calculation gives spurious results for the singlet reactance matrix elements. Let us fix the nonlinear parameter, e.g., at $\alpha=1$, and employ five basis functions ($N=5$). Then, from the general trend of the dashed lines of Fig. 2, one predicts the approximate regions around the wave numbers $k \approx 0.1$, 0.4, 0.8, and 1.3 a.u. where spurious behavior of the GNVM reactance matrix elements can be expected.

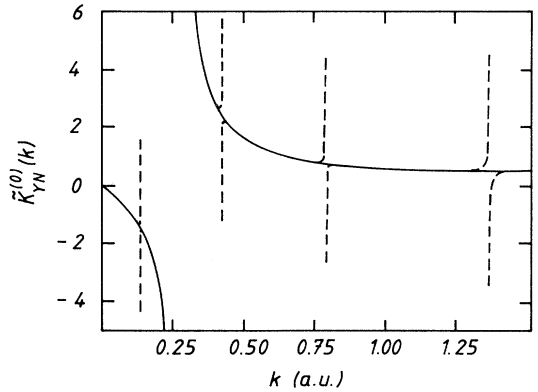

FIG. 3. Reactance matrix elements $\tilde{K}_{YN}^{(S)}$ computed by the generalized Newton variational method ($Y=G$, dashed curves) and its least-squares extension ($Y=L$, solid curves) for the singlet scattering process ($S=0$) at the fixed scale parameter $\alpha=1$ using basis-set size $N=5$, vs the wave number k within the range $0 \le k \le 1.5$ a.u. Apart from the regions where the dashed curves exhibit spurious behavior, both calculations give the same results within the width of line.

Figure 3 shows indeed that the GNVM reactance matrix elements $\tilde{K}_{GN}^{(0)}(k)=\tilde{K}_{GN}^{(0)}(5;k,1)$ illustrated by the dashed curves exhibit anomalous behavior at the wave numbers $k \approx 0.134$, 0.42, 0.79, and 1.37, near the ones predicted above. The width of these spurious singularities is broader at greater wave numbers (and much broader than in the case of triplet scattering discussed before). The solid curves represent the results $\tilde{K}_{LN}^{(0)}(k)=\tilde{K}_{LN}^{(0)}(5,5;k,1)$ obtained by the least-squares method [see Eq. (2.43)]. Both curves $\tilde{K}_{YN}^{(0)}$ ($Y=G,L$) reproduce the well-known (true) singularity structure of the singlet reactance matrix element at $k \approx 0.28$ a.u. Moreover, the least-squares results give the correct behavior also in the regions where the GNVM calculations yield unbounded values for the reactance matrix element.

Besides the spurious singularities, the GNVM exhibits another feature which may cause some trouble when concluding about the accuracy of the calculation from the convergence characteristics alone. Figure 4 illustrates the behavior of the singlet reactance matrix elements computed by the GNVM at $k=0.5$ a.u., with increasing basis-set size N in the parameter range $0.7<\alpha<10$. (In the omitted region $0<\alpha<0.7$ an obscure behavior of the computed reactance matrix element can be observed due to the appearance of the numerous spurious singularities). The functions $\tilde{K}_{GN}^{(0)}(N;0.5,\alpha)$ numbered by N in Fig. 4 show a convincing line of stability at the true value of 1.67 of the singlet reactance matrix element. However, one also observes a secondary plateau around 2.64 which is very stiff, still present at $\alpha \approx 100$ with $N=5$. The appearance of this stubborn spurious plateau (well-known [27,28,31] in the applications of the Kohn variational method) may lead one to draw quite a false conclusion when one is interested in the accuracy of the calculated results by inspecting the convergence characteristics.

Table I contains examples for this situation by listing GNVM results for the singlet reactance matrix element $\tilde{K}_{GN}^{(0)}(N;k,\alpha)$ at fixed wave number $k=0.5$ a.u., selected values of α, and different basis-set size N. If one performed the calculation only at one value of α (say, at

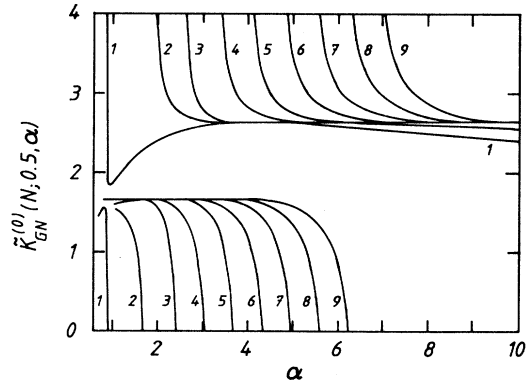

FIG. 4. Reactance matrix elements $\tilde{K}_{GN}^{(S)}$ computed by the generalized Newton variational method at $S=0$, $k=0.5$ a.u. vs the scale parameter α. The curves are numbered to identify the basis-set size N used.

TABLE I. Singlet reactance matrix element $\tilde{K}^{(0)}_{GN}(\alpha)$ computed by the generalized Newton variational method (GNVM) at fixed wave number $k=0.5$ a.u. and selected values of the scale parameter α. The size of the basis set is denoted by N.

N	$\tilde{K}^{(0)}_{GN}(1)$	$\tilde{K}^{(0)}_{GN}(3)$	$\tilde{K}^{(0)}_{GN}(5)$	$\tilde{K}^{(0)}_{GN}(7)$	$\tilde{K}^{(0)}_{GN}(9)$
1	1.8451	2.5802	2.6217	2.5431	2.4461
2	1.5489	2.6496	2.6296	2.6074	2.5651
3	1.5843	2.7842	2.6378	2.6421	2.6256
4	1.6459	0.2809	2.6567	2.6438	2.6396
5	1.6290	1.5680	2.7461	2.6439	2.6454
6	1.6467	1.6433	3.4831	2.6604	2.6455
7	1.6568	1.6667	−0.3306	2.7193	2.6474
8	1.6568	1.6689	1.3585	2.9433	2.6626
9	1.6619	1.6706	1.5716	4.0794	2.7052
10	1.6646	1.6706	1.6315	−1.0696	2.8216
11	1.6615	1.6707	1.6556	1.1449	3.1426
12	1.6667	1.6708	1.6642	1.4625	4.7235
13	1.6677	1.6708	1.6683	1.5738	−1.8389
14	1.6687	1.6708	1.6698	1.6215	0.9146
15	1.6686	1.6708	1.6705	1.6453	1.3427
16	1.6691	1.6708	1.6708	1.6571	1.4999

$\alpha=7$) within the fifth approximation ($N=5$), then one would accept the false value $\tilde{K}^{(0)}_{GN}=2.6439$ which seemed to be correct to four or five figures. [Similar observation can be made at $\alpha=9$ and basis size $N=6$. Note that use of $N\approx 5-6$ (distributed Gauss) basis functions per channel in GNVM benchmark calculations is justified by the experiences of Refs. [9] and [10]]. From Table I we learn also that the appropriate values of the scale parameter α lie approximately in the range $3\leq\alpha\leq 5$ for the GNVM. The rate of convergence is rather slow in comparison with the Schwinger variational method which provides the accurate result $\tilde{K}^{(0)}_{\text{Schwinger}}=1.670\,911\,2$ using basis-set sizes $N\geq 7$ (see Table I of Ref. [30]).

The secondary character of the convergence observed above can be recovered by performing least-squares calculations and monitoring the corresponding eigenvalues $\lambda^{(0)}_{LN}$ [see Eq. (2.41)] which have been listed in Table II. The slow decrease of the values of $\lambda^{(0)}_{LN}$ in the table clearly reflects the secondary nature of the convergence of the GNVM calculations in the critical regions ($\alpha=7$, $N\cong 5$; $\alpha=9$, $N\cong 6$). On the other hand, a rapid decrease of the values of $\lambda^{(S)}_{LN}(S=0,1)$ can be observed in the regions of α and N where the convergence is of primary nature.

Table III presents the LNVM results obtained for the singlet reactance matrix elements $\tilde{K}^{(0)}_{LN}(N,5;0.5,\alpha)$ at selected values of α and increasing basis-set size N. The

TABLE II. Measure of the error $\lambda^{(0)}_{LN}(\alpha)$ of the amplitude density calculated by the least-squares extension of the Newton variational method (LNVM) for singlet scattering at fixed wave number $k=0.5$ a.u. and selected values of the scale parameter α. The size of the basis set is denoted by N, and $N+5$ test functions are employed.

N	$\lambda^{(0)}_{LN}(1)$	$\lambda^{(0)}_{LN}(3)$	$\lambda^{(0)}_{LN}(5)$	$\lambda^{(0)}_{LN}(7)$	$\lambda^{(0)}_{LN}(9)$
1	5.4×10^{-1}	2.7×10^{-1}	9.4×10^{-4}	1.1×10^{-2}	1.6×10^{-2}
2	2.0×10^{-3}	7.2×10^{-1}	2.0×10^{-3}	5.5×10^{-4}	1.3×10^{-3}
3	5.6×10^{-4}	3.5×10^{-1}	3.4×10^{-3}	2.0×10^{-5}	6.0×10^{-5}
4	1.3×10^{-4}	2.8×10^{-3}	3.5×10^{-3}	5.9×10^{-5}	6.4×10^{-7}
5	6.7×10^{-6}	1.0×10^{-4}	6.0×10^{-3}	4.6×10^{-5}	1.3×10^{-6}
6	1.3×10^{-7}	4.1×10^{-6}	5.7×10^{-4}	2.6×10^{-5}	1.3×10^{-6}
7	1.7×10^{-7}	1.3×10^{-7}	1.4×10^{-5}	1.6×10^{-5}	6.4×10^{-7}
8	7.8×10^{-9}	5.6×10^{-9}	6.3×10^{-7}	3.6×10^{-5}	2.6×10^{-7}
9	3.2×10^{-10}	7.7×10^{-11}	3.7×10^{-8}	2.1×10^{-6}	1.1×10^{-7}
10	3.3×10^{-10}	1.7×10^{-12}	2.3×10^{-9}	4.4×10^{-8}	5.8×10^{-8}
11	1.0×10^{-11}	6.8×10^{-13}	1.4×10^{-10}	2.3×10^{-9}	1.2×10^{-7}
12	6.0×10^{-13}	6.2×10^{-12}	9.0×10^{-12}	1.4×10^{-10}	5.5×10^{-9}
13	1.5×10^{-13}	7.7×10^{-15}	5.3×10^{-13}	1.0×10^{-11}	1.3×10^{-10}
14	1.6×10^{-14}	5.0×10^{-16}	3.2×10^{-14}	7.5×10^{-12}	6.3×10^{-12}
15	9.8×10^{-16}	4.0×10^{-19}	1.7×10^{-15}	5.6×10^{-14}	4.2×10^{-13}
16	2.6×10^{-17}	1.3×10^{-18}	8.5×10^{-17}	4.3×10^{-15}	3.1×10^{-14}

TABLE III. Singlet reactance matrix element $\tilde{K}^{(0)}_{\mathrm{LN}}(\alpha)$ computed by the least-squares extension of the generalized Newton variational method (LNVM) at fixed wave number $k=0.5$ a.u. and selected values of the scale parameter α. The size of the basis set is denoted by N, and $N+5$ test functions are employed.

N	$\tilde{K}^{(0)}_{\mathrm{LN}}(1)$	$\tilde{K}^{(0)}_{\mathrm{LN}}(3)$	$\tilde{K}^{(0)}_{\mathrm{LN}}(5)$	$\tilde{K}^{(0)}_{\mathrm{LN}}(7)$	$\tilde{K}^{(0)}_{\mathrm{LN}}(9)$
1	1.9239	2.2962	2.6768	2.7532	2.7325
2	1.5370	2.5251	2.6529	2.6047	2.5874
3	1.5671	2.1425	2.5595	2.6416	2.6546
4	1.5744	1.4320	2.9142	2.6573	2.6417
5	1.6086	1.7085	3.4395	2.6400	2.6421
6	1.6365	1.6463	0.6315	2.7818	2.6550
7	1.6366	1.6764	1.4960	2.9839	2.6588
8	1.6500	1.6672	1.5727	4.9961	2.7357
9	1.6575	1.6713	1.6512	0.2855	2.8510
10	1.6572	1.6703	1.6527	1.2539	3.3284
11	1.6624	1.6705	1.6689	1.5120	5.9151
12	1.6648	1.6709	1.6670	1.5843	−0.2494
13	1.6671	1.6709	1.6710	1.6329	1.0903
14	1.6667	1.6707	1.6700	1.6470	1.3922
15	1.6677	1.6708	1.6711	1.6607	1.5277
16	1.6685	1.6708	1.6707	1.6637	1.5854

convergence characteristic of the LNVM results is similar to that of the GNVM calculations (see Table I). Also the accuracy of the two calculations compares well. Thus, the advantage of a LNVM calculation becomes manifest in the ability of avoiding spurious singularities (see Figs. 1 and 3) and indicating the unreliability of several apparently converged results included in Table I.

IV. COMMENTS

It is demonstrated that the generalized Newton variational method may present spurious singularities in the approximate static-exchange $\underline{K}$-matrix elements of the electron–hydrogen-atom scattering. This fact invalidates the general statement [2] about the anomaly-free character of the Newton variational method. Although the appearance of anomalies may depend on the choice of the basis sets, the theoretical conclusion of Ref. [22] should be supplemented by a careful analysis of the numerical results. We note the important remark of Ref. [34] on the possible occurrence of anomalies in the GNVM.

The spurious singularities of the GNVM show some similarity to both the well-studied [13,27,28] anomalies of the (real) Kohn variational method and the recently discovered [29–33] Schwinger anomalies. Using Slater-type basis functions, for example, the anomalies of the GNVM also appear in the case of purely attractive (or repulsive) potentials as in the Kohn method. On the other hand, the spurious singularities of the GNVM are located along those (spurious) zeros of the determinant $\bar{X}=\det|\langle\tilde{\varphi}_i|\mathcal{G}-\mathcal{G}U\mathcal{G}|\tilde{\varphi}_j\rangle|$ which are correlated with the zeros of the determinant $\bar{G}=\det|\langle\tilde{\varphi}_i|\mathcal{G}|\tilde{\varphi}_j\rangle|$. This feature is similar to the appearance of the Schwinger anomalies which arise due to the spurious zeros of $\det|\langle\tilde{\varphi}_i|U-U\mathcal{G}U|\tilde{\varphi}_j\rangle|$ lying close to the zeros of $\det|\langle\tilde{\varphi}_i|U|\tilde{\varphi}_j\rangle|$.

In summary, the anomalies of the GNVM appear in narrow regions of the wave number k and scale parameter α where the numerical results are affected radically (cf. Figs. 1, 3, and 4, and Table I). The least-squares extension presented in Sec. II is simply one way of getting smooth curves across the singular regions of k and α. By the prescription that the measure of the error of the amplitude density should decrease sufficiently as the size N of the basis-set is enlarged, one can hope to accept calculations at only one value of the scale parameter, thus saving a great deal of computational labor.

ACKNOWLEDGMENTS

This work has been supported by the OTKA under Grant Nos. 517/1990, 518/1990, and 2190/(I/3)/1991. One of us (B.A.) would like to thank Professor Erwin O. Alt for the pleasant and fruitful hospitality at the Gutenberg University of Mainz and the Deutschen Akademischen Austauschdienst (DAAD) for financially supporting a three-month visit to Germany in 1990. One of us (K.L.) would like to express his gratitude to Professor Béla Vasvári for the warm hospitality at the Institute of Physics, Technical University of Budapest, Hungary.

[1] R. G. Newton, *Scattering Theory of Waves and Particles*, 2nd ed. (Springer, Berlin, 1982), p. 321.
[2] I. H. Sloan and T. J. Brady, Phys. Rev. C **6**, 701 (1972).
[3] H. Rabitz and R. Conn, Phys. Rev. A **7**, 557 (1973); D. J. Kouri, J. Chem. Phys. **58**, 1914 (1973).
[4] T. J. Brady and I. H. Sloan, Phys. Rev. C **9**, 4 (1974).
[5] I. H. Sloan and S. K. Adhikari, Nucl. Phys. A **235**, 352 (1974); S. K. Adhikari and I. H. Sloan, *ibid.* **241**, 429 (1975).
[6] D. J. Kouri and F. S. Levin, Phys. Rev. C **11**, 352 (1975).
[7] G. Staszewska and D. G. Truhlar, Chem. Phys. Lett. **13**, 341 (1986).

[8] G. Staszewska and D. G. Truhlar, J. Chem. Phys. **86**, 2793 (1987).
[9] D. W. Schwenke, K. Haug, D. G. Truhlar, Y. Sun, J. Z. H. Zhang, and D. J. Kouri, J. Phys. Chem. **91**, 6080 (1987).
[10] D. W. Schwenke, K. Haug, M. Zhao, D. G. Truhar, Y. Sun, J. Z. H. Zhang, and D. J. Kouri, J. Phys. Chem. **92**, 3202 (1988).
[11] B. Ramachandran, T. -G. Wei, and R. E. Wyatt, Chem. Phys. Lett. **151**, 540 (1988).
[12] B. Ramachandran, T. -G. Wei, and R. E. Wyatt, J. Chem. Phys. **89**, 6785 (1988).
[13] M. Mladenovic, M. Zhao, D. G. Truhlar, D. W. Schwenke, Y. Sun, and D. J. Kouri, J. Phys. Chem. **92**, 7035 (1988).
[14] M. Mladenovic, M. Zhao, D. G. Truhlar, D. W. Schwenke, Y. Sun, and D. J. Kouri, Chem. Phys. Lett. **146**, 358 (1988).
[15] Y. Sun, C. Yu, D. J. Kouri, D. W. Schwenke, P. Halvick, M. Mladenovic, and D. G. Truhlar, J. Chem. Phys. **91**, 1643 (1989).
[16] D. Belkić and H. S. Taylor, Phys. Rev. A **39**, 6134 (1989).
[17] D. J. Kouri and D. G. Truhlar, J. Chem. Phys. **91**, 6919 (1989).
[18] M. Zhao, D. G. Truhlar, D. J. Kouri, Y. Sun, and D. W. Schwenke, Chem. Phys. Lett. **156**, 281 (1989).
[19] Y. Sun, D. J. Kouri, D. G. Truhlar, and D. W. Schwenke, Phys. Rev. A **41**, 4857 (1990).
[20] B. Ramachandran, M. D'Mello, and R. E. Wyatt, J. Chem. Phys. **93**, 8110 (1990).
[21] Y. Sun, D. J. Kouri, and D. G. Truhlar, Nucl. Phys. A **508**, 41c (1990).
[22] H. -D. Meyer, J. Horáček, and L. S. Cederbaum, Phys. Rev. A **43**, 3587 (1991).
[23] M. A. Abdel-Raouf, Phys. Rep. **108**, 1 (1984).
[24] B. R. Johnson and D. Secrest, J. Math. Phys. **7**, 2187 (1966); M. Baer and D. J. Kouri, Phys. Rev. A **4**, 1924 (1971).
[25] K. Takatsuka, R. R. Lucchese, and V. McKoy, Phys. Rep. **131**, 147 (1986).
[26] K. Takatsuka and V. McKoy, Phys. Rev. A **23**, 2352 (1981); K. Takatsuka, R. R. Lucchese, and V. McKoy, Phys. Rev. A **24**, 1812 (1981).
[27] C. Schwartz, Ann. Phys. (N.Y.) **16**, 36 (1961); Phys. Rev. **124**, 1468 (1961); *ibid.* **141**, 1468 (1966).
[28] R. K. Nesbet, *Variational Methods in Electron-Atom Scattering Theory* (Plenum, New York, 1980).
[29] B. Apagyi, P. Lévay, and K. Ladányi, Phys. Rev. **37**, 4577 (1988).
[30] K. Ladányi, P. Lévay, and B. Apagyi, Phys. Rev. A **38**, 3365 (1988).
[31] P. Lévay and B. Apagyi, J. Phys. B **21**, 3741 (1988).
[32] C. Winstead and V. McKoy, Phys. Rev. A **41**, 49 (1990).
[33] S. K. Adhikari, Phys. Rev. A **42**, 6 (1990).
[34] W. H. Miller, Annu. Rev. Phys. Chem. **41**, 245 (1990).
[35] G. A. Erskine and H. S. W. Massey, Proc. R. Soc. London Ser. A **212**, 521 (1952).
[36] J. A. Shohat and J. D. Tamarkin, *The Problem of Moments* (American Mathematical Society, New York, 1943).
[37] B. Apagyi and K. Ladányi, Phys. Rev. A **33**, 182 (1986).
[38] K. Ladányi and T. Szondy, Nuovo Cimento B **5**, 70 (1971).
[39] K. Ladányi, Nuovo Cimento A **61**, 173 (1969).